

Experimental study on gas production and solution composition during the interaction of femtosecond laser pulse and liquid

Yichun Wang(王奕淳)1, Han Wu(吴寒)1;†, Wenkang Lu(陆文康)1, Meng Li(李萌)2, Ling Tao(陶凌)3, and Xiuquan Ma(马修泉)1;2

Citation: Chin. Phys. B, 2022, 31 (**7**): 070204. DOI: 10.1088/1674-1056/ac7449
Journal homepage: http://cpb.iphy.ac.cn; http://iopscience.iop.org/cpb

What follows is a list of articles you may be interested in

Modes decomposition in particle-in-cell software CEMPIC

Aiping Fang(方爱平)†, Shanshan Liang(梁闪闪), Yongdong Li(李永东), Hongguang Wang(王洪广), and Yue Wang(王玥)
Chin. Phys. B, 2020, 29 (**10**): 100205. DOI: 10.1088/1674-1056/abaed6

Nonlinear radiation response of n-doped indium antimonide and indium arsenide in intense terahertz field

Jiao-Li Gong(龚姣丽), Jin-Song Liu(刘劲松), Zheng Chu(褚政), Zhen-Gang Yang(杨振刚), Ke-Jia Wang(王可嘉), Jian-Quan Yao(姚建铨)
Chin. Phys. B, 2016, 25 (**10**): 100203. DOI: 10.1088/1674-1056/25/10/100203

Carlson iterating rational approximation and performance analysis of fractional operator with arbitrary order

Qiu-Yan He(何秋燕), Bo Yu(余波), Xiao Yuan(袁晓)
Chin. Phys. B, 2017, 26 (**4**): 040202. DOI: 10.1088/1674-1056/26/4/040202

SPECIAL TOPIC — Laser and plasma assisted synthesis of advanced nanomaterials in liquids

Experimental study on gas production and solution composition during the interaction of femtosecond laser pulse and liquid

Yichun Wang(王奕淳)[1], Han Wu(吴寒)[1,†], Wenkang Lu(陆文康)[1], Meng Li(李萌)[2], Ling Tao(陶凌)[3], and Xiuquan Ma(马修泉)[1,2]

[1] *The State Key Laboratory of Digital Manufacturing Equipment and Technology, School of Mechanical Science and Engineering, Huazhong University of Science and Technology (HUST), Wuhan* 430074, *China*

[2] *Guangdong Intelligent Robotics Institute, Dongguan* 523808, *China*

[3] *Department of Cardiology, Xijing Hospital, The Fourth Military Medical University, Xi'an* 710032, *China*

(Received 5 November 2021; revised manuscript received 23 May 2022; accepted manuscript online 29 May 2022)

The process of ionizing normal saline induced by femtosecond laser is studied from the perspective of gas production rate and composition. When the repetition rate is less than 1000 Hz, each laser pulse independently generates ionization gas. At the same time, we discovered the inhibitory effect of meglumini diatrizoici on the ionization process and explained the reasons for this inhibition. Finally, the gas composition proved that the primary gas production mechanism of the femtosecond laser is the decomposition of water molecular, and the composition of the solution after the reaction proved the decomposition effect of the laser on meglumine.

Keywords: femtosecond laser，ionization，gas production rate, meglumini diatrizoici

PACS: 02.30.Uu, 02.30.Vv, 06.20.Dk, 06.60.–c **DOI:** 10.1088/1674-1056/ac7449

1. Introduction

The idea of recanalization of occluded arteries by non-surgical methods has been around for a long time. In 1964, Dotter and Judkins first proposed the treatment of atherosclerotic occlusion with catheter recanalization technology.[1] Balloon recanalization has been widely used to treat peripheral artery and coronary artery stenosis and occlusion for many years.[2] In the 1980s, continuous-wave lasers were used for laser ablation technology, brought about carbonization occurring in surrounding tissues due to high thermal input.[3] In the 1990s, pulse lasers of the millisecond[4] and the nanosecond[5] scale were used to ablate thrombus. However, millisecond laser ablation was limited by the special design of the catheter, which made it difficult to reach the occlusion site. The millimeter-scale ionization created by nanosecond pulses can cause damage to blood vessel walls. The typical size of the particles generated in femtosecond laser ablation of tissue is in the submicron scale, which minimizes the risk of blocking downstream capillaries. Furthermore, the linear absorption thresholds of thrombus and vessel differ by nearly an order of magnitude in the ultraviolet and visible spectra. It can safely ablate the thrombus material without accidentally damaging the vessel wall.[6] With these advantages, the femtosecond pulse laser have a potential to become the primary light source for the next generation of intravascular plaque ablation.[7]

When an ultrafast laser pulse is shot in a liquid environment, the laser induces the formation of bubbles.[8–12] However, there are significant differences in gas generation induced by femtosecond laser and laser with more extended pulse width. The chemical ionization of water molecules becomes the primary inducement for the gas generation induced by femtosecond laser.[13] At present, nanosecond laser is still the primary source of laser ablation.[14,15] Therefore, the femtosecond laser ionization mechanism research will provide a strong theoretical basis for the next generation of laser coronary angioplasty.

The ionization process induced by femtosecond pulse laser is studied experimentally from the perspectives of gas production rate and composition analysis. The study of gas generation rate can explore the influence of different factors on femtosecond laser induced ionization process. The analysis of the composition can be used to study the mechanism of femtosecond pulse laser ionization process and the additional reaction accompanying the ionization process.

2. Experiment setup

As shown in Fig. 1, the experimental platform was designed for femtosecond laser ionization experiments. During the experiment, the liquid involved in the experiment is loaded into the reaction unit, where femtosecond pulse laser is focused. And the focused femtosecond pulsed laser would break down the studied liquid environment and produce ionization gas. The reaction unit is housed in a black chamber to isolate stray light and allow the spectrometer to collect the light produced by the laser-induced plasma.

[†]Corresponding author. E-mail: hanwu@hust.edu.cn

© 2022 Chinese Physical Society and IOP Publishing Ltd

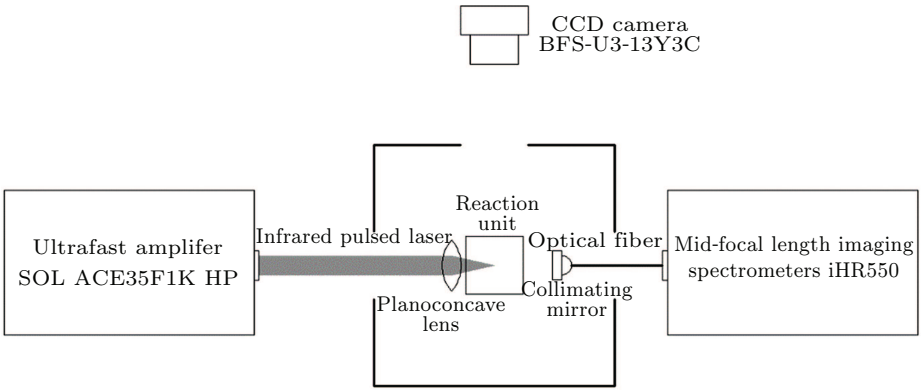


Fig. 1. External structure diagram of the experimental platform for laser-induced plasma spectroscopic analysis.

The femtosecond laser amplifier used in this experiment is SOLSTICE ACE35F1K HP, with pulse laser frequency of 1000 Hz, the wavelength of 800 nm, the pulse width of 35 fs, beam quality factor M2 of 1.25, spot diameter of 11 mm, and the highest attainable pulse energy of 5 mJ. The lens model used in the focusing process is LA1951-B, with a focal length of 25.4 mm. The CCD camera model is BFS-U3-13Y3C, and its lens model is FA5002A-Spec-V2. The optical fiber used to collect the light source of laser-induced plasma is MKSM-VIS-600-3m, and the spectrometer used to analyze the spectrum is iHR550, with the scan range of 0 nm–1500 nm, step size of 0.002 nm, scanning speed of 160 nm/s.

The reaction unit is a self-made setup. The setup is made of quartz glass and has a total volume of about 182 ml. The specific use method of this setup can be referred to in the appendix at the end of the paper.

3. Result and discussion

3.1. Determination of threshold and discussion on the mechanism of femtosecond laser-induced ionization of normal saline

We use the method shown in the appendix to measure the gas production rate of the ionization process of the normal saline at different average power at the repetition rate of 1000 Hz. The result is shown in Fig. 2.

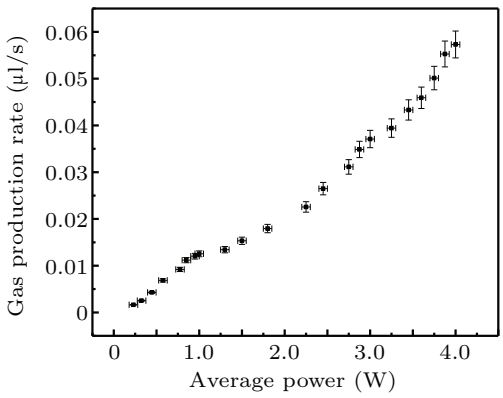


Fig. 2. The relationship between gas productivity and average power.

The transverse error in Fig. 2 is the reading error of the power meter. A total of 22 groups of different parity power were set up in the experiment. Each group had five measurements of the ionization gas production rate and averaged the measurement results. The longitudinal error in the figure was the standard deviation.

As shown from Fig. 2, with the increase of average power, the generation rate of ionization gas also increases. The process of ionization gas production rate increasing with laser average power can be roughly divided into three stages. When the laser average power is less than 1 W, the production rate of ionization gas has a linear relationship with the average power, and the growth rate is relatively fast. When the laser average power is between 1 W and 2.5 W, the production rate of ionization gas appears a plateau with the increase of the average power of laser, and the growth rate becomes slow. When the laser average power is greater than 2.5 W, the production rate of ionization gas increases rapidly and linearly again.

Based on the above findings, we speculate that the phenomenon may be caused by the following reasons. First, when the average laser power is between 1 W and 2.5 W, the position far from the focus has not ionized, but the position near the focus has reached the upper limit of ionized gas. Second, based on the first reason, bubbles generated near the focus are too dense, and there is mutual influence in the process of bubble expansion.

The repetition frequency set in this experiment can be adjusted multiple times, up to 1000 Hz. The adjustment of pulse laser repetition rate only changes the number of pulses per unit time and does not change the energy of each pulse. In order to conduct comparative experiments, four groups of experiments under the conditions of 0.85 mJ, 1.5 mJ, 2.25 mJ, and 3 mJ single pulse energies were selected. The experimental method is the same as above, and the result is shown in Fig. 3. The experimental groups corresponding to the four straight lines in Fig. 3 were 0.85 mJ, 1.5 mJ, 2.25 mJ, and 3 mJ respectively from bottom to top. For each experiment corresponding to pulse energy, we selected three groups of experiments with

repetition frequencies of 250 Hz, 500 Hz, and 1000 Hz.

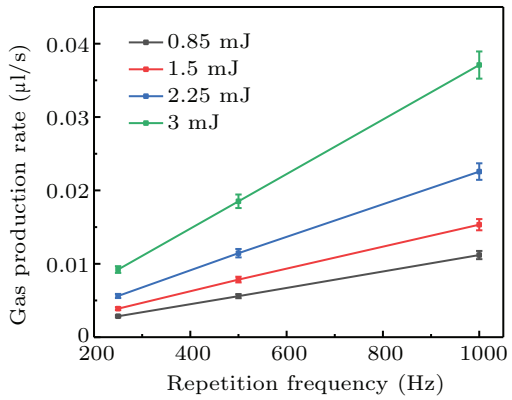


Fig. 3. The relationship between gas productivity and repetition frequency.

It can be concluded from Fig. 3 that under the same repetition frequency, the production rate of ionization gas increases with the increase of laser single pulse energy, which is consistent with the previous conclusion. In the case of the same single pulse energy, the production rate of ionization gas is proportional to the repetition rate of the laser. Therefore, each laser pulse independently generates ionization gas when the repetition frequency is less than 1000 Hz.

The gases generated by ionization in the experiment were collected and analyzed by GC2020 gas chromatograph. It is found that 21.67% of the ionization gas is hydrogen, 10.84% of the ionization gas is oxygen, and the rest is water vapor. Therefore, the femtosecond pulsed laser-induced ionization process is essentially different from the nanosecond pulsed laser-induced ionization process. The nanosecond pulsed laser-induced ionization process is not only a physical phase transition process, but also a chemical decomposition of water molecules.[13] The decomposition of water accompanies the femtosecond pulsed laser-induced ionization process into hydrogen and oxygen, which is irreversible. Hence, there is a stable gas generation rate in this process.

3.2. Study on the influence of meglumini diatrizoici on ionization process and its causes

In the angioplasty process, the contrast medium and x-ray are commonly used to visualize the vascular system. Therefore, the interacting mechanism between the femtosecond laser pulse and contrast solution has important value. Meglumini diatrizoici is a contrast medium commonly used in angioplasty. In the subsequent experiments, we mainly focused on the sample of meglumini diatrizoici.

The meglumini diatrizoici used in our experiment was prepared by dissolving meglumine in physiological saline. The sample solution is available in three concentrations: 1 g/L, 2 g/L, and 5 g/L.

The gas production rate in the meglumini diatrizoici induced by femtosecond laser ionization was measured according to the experimental method described above. We set the repetition frequency of the pulsed laser to 1000 Hz and selected four different pulse energies of 1 mJ, 1.5 mJ, 2.25 mJ, and 3 mJ. The experimental results are shown in Fig. 4. The experimental groups corresponding to the four curves in Fig. 4 were 1 mJ, 1.5 mJ, 2.25 mJ, and 3 mJ respectively from bottom to top. For each experiment corresponding to pulse energy, we selected four groups of experiments with the concentration of the meglumini diatrizoici of 0 g/L(pure normal saline), 1 g/L, 2 g/L, and 5 g/L, respectively.

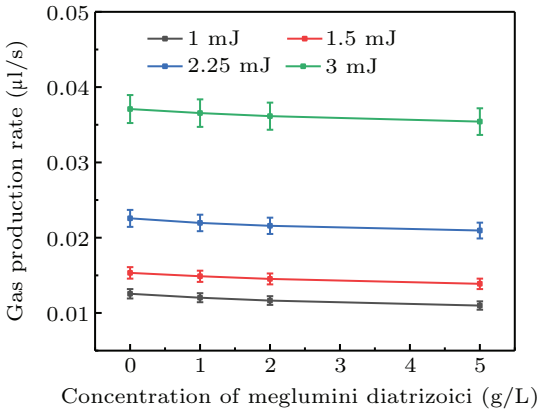


Fig. 4. The relationship between gas productivity and concentration of the meglumini diatrizoici.

As can be seen from Fig. 4, for the same concentration of meglumini diatrizoici, the higher the pulse energy of the laser, the higher the gas production rate. For the same pulse energy, the higher the concentration of meglumini diatrizoici, gas production rate will have a slight decrease. It can be concluded from Fig. 4 that meglumine has a specific inhibitory effect on the femtosecond laser-induced ionization process, and the higher solution concentration, the more pronounced the inhibitory effect. We have conducted the t-test on the values at each concentration relative to 0 g/L for the same pulse energy to determine statistical significance. We found that the meglumini diatrizoici of 1 g/L has a significant effect on the gas production rate with 75% confidence; the meglumini diatrizoici of 2 g/L has a significant effect on the gas production rate with 90% confidence; and the meglumini diatrizoici of 5 g/L has a significant effect on the gas production rate with 97.5% confidence. We found that with the increase of the concentration of meglumini diatrizoici, the confidence of its effect on gas production rate also increased. When the concentration of meglumini diatrizoici was 5 g/L, its confidence was statistically significant.

In order to explore the reason for this phenomenon, we used the iHR550 spectrometer to analyze the spectrum of the plasma generated by femtosecond laser focusing on the meglumini diatrizoici. The light excited by the laser-induced plasma was collected and introduced into the spectrometer by collimating mirror and optical fiber during the experiment. We cut off the spectrum at 650 nm because the direct 800-nm

emission overwhelms the small changes observed in the region from 400 nm–650 nm, and the results are shown in Fig. 5.

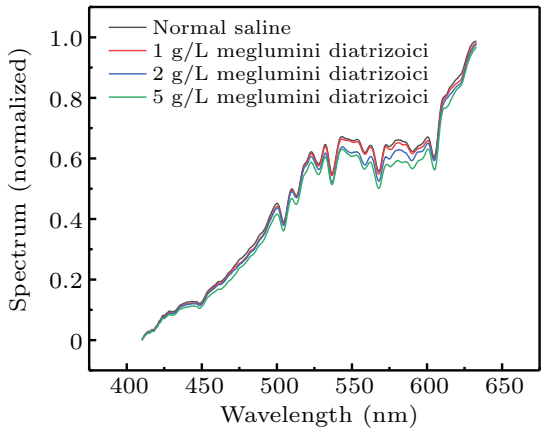


Fig. 5. The spectral distribution of light excited by a laser-induced plasma in samples of meglumini diatrizoici and physiological saline.

As demonstrated in Fig. 5, the spectrum was suppressed with increased concentration of meglumini diatrizoici, due to meglumine diatrizoate organic molecules can capture the electrons in the plasma and suppress the spectrum of the plasma.[16–18]

The essence of plasma generation is laser ionization of water, which is also the basis of the femtosecond laser-induced ionization process. Meglumine capture the electrons in the plasma, thereby inhibiting the decomposition of water into hydrogen and oxygen, and reducing ionization gas production rate. It also proved that femtosecond pulsed laser-induced ionization is an ionization process of water molecules.

3.3. Reaction process and component analysis of meglumini diatrizoici

A high-resolution liquid mass spectrometer was used to analyze the meglumini diatrizoici before and after laser ablation. The only organic molecule in the solution before laser ablation is meglumine diatrizoate (as shown in Fig. 6(a)). This indicates that meglumine diatrizoate is dissolved in the form of a primitive molecule. In the solution after laser ablation, we additionally found four organic molecules, as shown in Figs. 6(b), 6(c), 6(d), and 6(e).

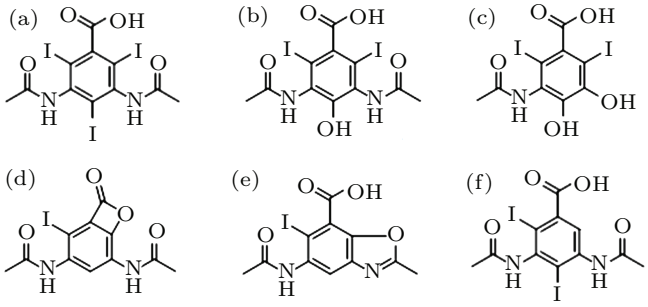
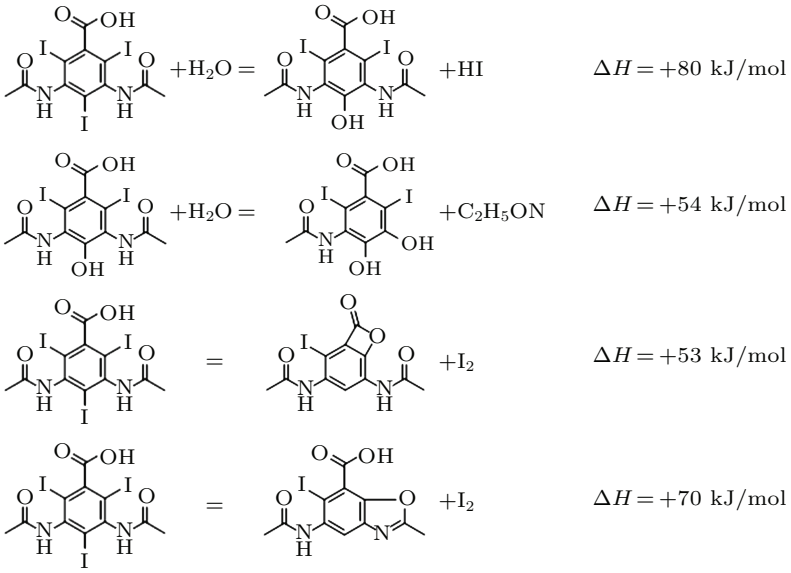


Fig. 6. Molecular structure analysis results of the high-resolution liquid mass spectrometer: (a) the sample before laser ablation, (b)–(e) the excess samples after laser ablation, and (f) the sample after the reaction with H_2O_2.

According to the balance of chemical equation, the following four chemical reactions has been obtained:



After the experiment, the meglumini diatrizoici was pale yellow, and it is the color of the by-products of the reaction I_2 and HI that dissolved in water.

The enthalpy changes of the above four reactions are all positive, which are endothermic reactions. It indicates that the addition of meglumine diatrizoate will cause the pulse laser to share part of the light energy to participate in the decomposition reaction of meglumine diatrizoate itself, resulting in the reduction of the light energy converted into bubble energy. Bubble energy is a necessary condition for ionization.[19,20] Therefore, this is another reason why meglumine diatrizoate inhibits the rate of ionization gas production.

The essential process of the ionization of water into hydrogen and oxygen is that photons break H_2O to form –OH

and –H, then broken by photons to form –O and –H, and then –O and –O combine to form O_2, –H and –H combines to form H_2.[13] Based on the above mentioned first and second reactions, we conjecture the –OH and –H generated by the ionization of water may participate in the decomposition reaction of meglumine diatrizoate in advance, and combine with the organic molecules of meglumine diatrizoate, fail to complete the subsequent reaction to generate H_2 and O_2. In order to verify the above conjecture, the GC2020 gas chromatograph was used to detect the gas components produced by femtosecond pulsed laser induced ionization in the meglumini diatrizoici. The results are shown in Table 1.

Table 1. Proportion of hydrogen in the cavitating gas in the meglumini diatrizoici with different concentrations.

Concentration of meglumini diatrizoici (g/L)	0	1	2	5
Proportion of hydrogen (%)	21.67	20.33	19.24	18.83

As can be seen from Table 1, the hydrogen proportion in laser-induced ionization gas gradually decreases with the increase of the concentration of the meglumini diatrizoici. Thus, the decomposition reaction of meglumine diatrizoate consumes part of the –OH and –H generated by water ionization.

In the decomposition of water into hydrogen and oxygen, there is the long-lived product H_2O_2. In order to prove that the four products we found were not caused by the reaction of H_2O_2 and meglumine, we also conducted a control experiment. We directly mixed the corresponding amount of H_2O_2 and meglumini diatrizoici to react, and then tested the reaction products again with high-resolution liquid mass spectrometer. In this sample, we found only one reaction product Fig. 6(f). Basically, it could be judged that the four products Figs. 6(b), 6(c), 6(d), and 6(e) were generated by the decomposition of meglumine molecules caused by laser. Of course, we do not rule out that product Fig. 6(f) is an intermediate product of Fig. 6(b) or Fig. 6(c), but the subsequent reaction process can only be induced by the laser.

The addition of meglumine does inhibit the decomposition of water into hydrogen and oxygen, which is the third reason that meglumine can inhibit the generation of ionization gas induced by femtosecond laser.

4. Conclusion and perspectives

In conclusion, we used a self-made experimental method to measure the gas formation rate during femtosecond pulse-induced ionization. We find that each pulse generates ionization gas independently when the repetition rate of the pulsed laser is more minor than 1000 Hz.

The gas composition of physiological saline after femtosecond laser-induced ionization was measured. We found that the nature of femtosecond laser-induced ionization is a decomposition of water into hydrogen and oxygen.

We found that the introduction of meglumine can inhibit the ionization process, and the inhibition effect is more evident with higher concentration. The first reason is that the meglumine diatrizoate organic molecules have an adsorption effect on the photoinduced plasma, which inhibits the ionization process of water molecules. The second reason is that the chemical reaction of meglumine with the pulsed laser is endothermic, which distributes some of the light energy used for ionization. The third reason is that it consumes some of the free –OH and –H in chemical reactions, which inhibit the decomposition of water molecules into hydrogen and oxygen.

Acknowledgements

Project supported by the National Natural Science Foundation of China (Grant No. 81927805) the Fundamental Research Funds for the Central Universities of HUST (Grant No. 2019kfyXKJC062), the Guangdong Major Project of Basic and Applied Basic Research (Grant No. 2019B030302003), the Science and Technology Planning Project of Guangdong Province, China (Grant No. 2018B090944001), and China Postdoctoral Science Foundation (Grant No. 2018M632837).

Thanks to professor Shiyuan Liu and professor Hao Jiang's research group for their strong support of the experiment involved in this paper, especially thanks to Doctor Zhicheng Zhong and Doctor Jiamin Liu for their help in the experiment process.

In addition, we would like to express our deep gratitude to the Analytical & Testing Center of Huazhong University of Science and Technology for their friendly cooperation.

Appendix A: The specific used method of the self-made setup

The self-made setup used the drainage method to measure the production rate of ionization gas and converts the volume of ionization gas induced by pulse laser into the height of liquid level rise in the capillary.[21,22] The specific operation method is expressed as follows:

Step 1 Install the constant volume capillary in the left hole and add the liquid.

Step 2 After the setup is filled with liquid, mark the liquid level in the capillary (Fig. A1(a)). Because it is a capillary, the liquid level is higher than the others. According to the principle of the connector, the liquid pressure at both ends of the opening and the top of the setup is one bar.

Step 3 Seal the other end and keep the capillary liquid level below the marked position.

Step 4 The ionization process begins. With the formation of ionization bubbles, the liquid level in the capillary will rise. Because the density of ionization gas is less than water, the ionization bubbles also rise to the top of the setup (Fig. A1(b)).

Step 5 When the liquid level in the capillary rise to the marked position, stop the ionization. Now, the bubbles gather at the top of the setup (Fig. A1(c)). Because of it, the pressure of the ionization gas is one bar.

Step 6 Gain the rising height and time of liquid level. We can get the gas production rate (the capillary used in the experiment is a constant volume capillary). The pressure and temperature of the cavitating gas are obtained. Hence, the rate is not only a volume rate but also a mol rate.

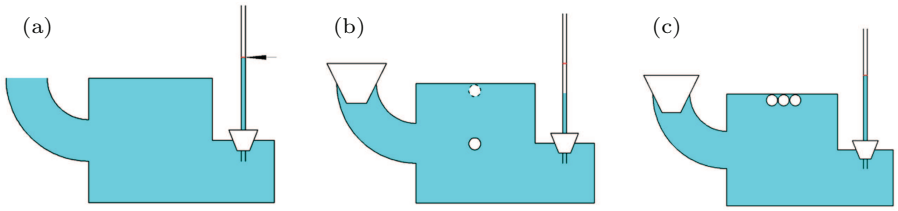


Fig. A1. The specific operation method.

References

[1] Dotter C T and Judkins M P 1964 *Circulation* **30** 654
[2] Kitrell C, *et al*. 1985 *Appl. Opt.* **25** 2280
[3] Strikwerda S, Bott-Silverman C, Ratliff N B, *et al*. 1988 *Lasers Surg. Med.* **8** 66
[4] Heijer P, Dijk R B, Pentinga M L, Hillege H L and Lie K I 1994 *J. Intervent. Cardiol.* **7** 525
[5] van Leeuwen T G, van Erven L, Meertens J H, Motamedi M, Post M J and Borst C 1992 *J. Am. Coll. Cardiol.* **19** 1610
[6] Tan S, Wu J J, Huang Q, *et al*. 2019 *Acta Phys. Sin.* **68** 057901 (in Chinese)
[7] Liu M N, Li M T, Yang H, *et al*. 2018 *Chin. Phys. B* **27** 094212
[8] Alfred Vogel, Norbert Linz, Sebastian Freidank and Günther Paltauf. 2008 *Phys. Rev. Lett.* **100** 038102
[9] Chen S, Zhang D, Wang C H, *et al*. 2019 *Acta Phys. Sin.* **68** 074301 (in Chinese)
[10] Feng K Y and Wang C H 2019 *Acta Phys. Sin.* **68** 244301 (in Chinese)
[11] Shen Z Z 2020 *Chin. Phys. B* **29** 014304
[12] Sun J, Shen Z Z and Mo R Y 2019 *Chin. Phys. B* **28** 014301
[13] Hanna Kierzkowska-Pawlak, Jacek Tyczkowski, Arkadiusz Jarota and Halina Abramczyk 2019 *Appl. Energy* **247** 24
[14] Herzog A, Steinberg I and Ishaaya A A 2017 *J. Biophoton.* **10** 1262
[15] Herzog A, Steinberg I, Gaisenberg E, Nomberg R and Ishaaya A A 2016 *J. Sel. Top. Quantum* **22** 1
[16] Li H, Shi Z, Wang X W, Sui L Z, Li S Y and Jin M X 2017 *Chem. Phys. Lett.* **681** 86
[17] Zhang K J, Liu L, Zeng Q W, *et al*. 2019 *Acta Phys. Sin.* **68** 194207 (in Chinese)
[18] Wang Y L, Zhao B, Min C J, *et al*. 2020 *Chin. Phys. B* **29** 027302
[19] Venugopalan V, Guerra A, Nahen K and Vogel A 2002 *Phys. Rev. Lett.* **88** 078103
[20] Vogel A and Busch S 1996 *J. Acoust. Soc. Am.* **100** 148
[21] Davis G S, Bott-Silverman C, Goormastic M, Gerrity R G, Kittrell C, Feld M and Kramer J R 1988 *Lasers Surg. Med.* **8** 72
[22] Appelman Y E, Piek J J, Verhoofstad G G, Gijsbers G H and van Gemert M J 1996 *Lasers Surg. Med.* **18** 197